Application of a Numerical Moving Boundary Model for Prediction of Bubble Growth Rate in Boiling of Pure Liquids and Miscible Binary Mixture

Dr. Ali Hussain Tarrad
Mechanical Engineering Dept., College of Engineering
Al-Mustansiriya University, Baghdad, Iraq

Abstract

This investigation deals with the estimation of bubble growth rate during nucleate pool boiling of pure liquids and miscible wide boiling range binary mixture such as n-Pentane/Tetradecene mixture. Understanding the process of heat exchange between the heating surface and the adjacent liquid during boiling should start from the ability to understand the mechanism of bubble growth rate and departure parameters (diameter and frequency). For binary mixtures, the mass balance of the more volatile component (n-Pentane) and energy balance at the vapor/liquid interface were used to predict the bubble radius, R(t), as a function of time. Whereas, for pure liquids the energy balance at the bubble boundary was used to estimate the bubble radius together with the temperature distribution in the liquid domain.

The bubble growth rate of binary mixtures predicted by this model was compared with existing theories. The discrepancy in the bubble growth constant between this analysis and those of other investigators was explained and verified by the present model. The model of pure liquids showed well agreement with available experimental data.

الخلاصـــة

*البحث يتعامل مع التخمين النظري لمعدل نمو الفقاعة خلال الغليان الحوضي للسوائل النقية أو الخلائط الثنائية المتجانسة مثل بنتان/تتراديكان. إن فهم عملية التبادل الحراري بين السطح الساخن وطبقة السائل المتاخمة له أثناء عملية الغليان تبدأ من إمكانية فهم النظام القائم لمعدل نمو الفقاعة والعوامل الداخلة والمؤثرة عند الانفصال من السطح (القطر والتكرار خلال الثانية الواحدة). في حالة الخلائط المتجانسة فقد تم استخدام الاتزان الكتلي للعنصر الأكثر تطايراً (البنتان) ضمن مكونات الخليط عند جدار الفقاعة (السطح الفاصل بين السائل والبخار) والاتزان الحراري لغرض التنبؤ لنصف قطر الفقاعة بدلالة الزمن، **R(t)**. أما في حالة السوائل النقية فإن الاتزان الحراري عند جدار الفقاعة قد تم استخدامه للتنبؤ بقيمة **R(t)** وكذلك إيجاد التوزيع الحراري خلال السائل المجاور للفقاعة.*

معدل نمو الفقاعة المتولدة خلال الغليان الحوضي والمحسوب بواسطة هذا البحث قد تم مقارنته مع النظريات المتوفرة في هذا المجال. الاختلاف بمعدل نمو الفقاعة للخلائط المتجانسة والمحسوب بهذا البحث عن تلك المحسوبة باستخدام النظريات المتوفرة قد تم تفسيره وإثبات صحته بين طيات البحث. النموذج الخاص بالسوائل النقية قد أظهر مطابقة بصورة جيدة مع النتائج العملية المتوفرة.

1. Introduction

The asymptotic bubble growth stage is the dominant period of the bubble life, since the earlier stage, which is controlled by inertia and surface tension forces, occupies a very short period. Rayleigh [1], obtained the velocity at the boundary at the liquid/vapor interface of inviscid and incompressible liquid with uniform pressure in the form:

$$(\dot{R})^2 = \frac{2p_\infty}{3\rho_l}\left(\frac{R_0^{\,3}}{R^3} - 1\right) \quad \text{..... (1)}$$

and the equation of motion as:

$$\rho_\ell\left[R\ddot{R} + \frac{3}{2}(\dot{R})^2\right] = p(R) - p_\infty \quad \text{..... (2)}$$

Plesset and Zwick [2], took into consideration the cooling effect caused by the vaporization at the bubble boundary. Their formula of bubble growth rate has the expression:

$$R = \left(\frac{12}{\pi}\right)^{1/2} J(at)^{1/2} \quad \text{..... (3.a)}$$

where:

$$J = \frac{\rho_l C_{pl}(T_0 - T_S)}{\rho_\upsilon h_{fg}} \quad \text{..... (3.b)}$$

Forster and Zuber [3], extended the Rayleigh equation and using the Clausius-Clapeyron relation:

$$\Delta T = \frac{T(\vartheta_\upsilon - \vartheta_l)}{h_{fg}}[p(R) - p_\infty] \quad \text{..... (4)}$$

To introduce the temperature difference, $\Delta T=[T(R) - T_{S\infty}]$, to the equation. Here, $T_{S\infty}$ is the saturation temperature corresponding to the pressure p_∞. The final form of their formula is:

$$\dot{R} = \frac{\Delta T C_{pl}\rho_l(\pi a)^{1/2}}{h_{fg}\rho_\upsilon}\,\frac{1}{2t^{1/2}} \quad \text{..... (5)}$$

Scriven [4], in an analysis of bubble growth rate in pure and binary liquid mixtures took into account the radial convection effect on the bubble growth which results from the unequal densities of the liquid and vapor phases, convection effect.

The energy equation which determines the temperature distribution in the liquid for incompressible fluid with no viscous dissipation and no energy fluxes other than ordinary heat conduction was expressed as:

$$\frac{\partial T}{\partial t} = a[\frac{\partial^2 T}{\partial\, r^2} + \frac{2}{r}\frac{\partial T}{\partial r}] - \frac{\varepsilon R^2 \dot{R}}{r^2}\frac{\partial T}{\partial r} + \frac{Q}{\rho_l C_{pl}} \quad \text{..... (6.a)}$$

The mass balance equation for the more volatile component for constant and uniform liquid density, constant diffusivity and no mass fluxes other than ordinary diffusion, was written as follows:

$$\frac{\partial C}{\partial t} = D[\frac{\partial^2 C}{\partial r^2} + \frac{2}{3}\frac{\partial C}{\partial r}] - \frac{\varepsilon R^2 \dot{R}}{r^2}\frac{\partial C}{\partial r} \quad \text{..... (6.b)}$$

Scriven solved eq.(6) for pure liquids and binary mixtures with bubble growth rate expression in the form:

$$R(t) = 2\beta(at)^{1/2} \quad \text{..... (7)}$$

with:

$$R(t) = (\frac{12}{\pi})^{1/2}[\frac{\Delta T\sqrt{\rho_l C_{pl} kt}}{\rho_\upsilon\{h_{fg} + (C_{pl} - C_{p\upsilon})\Delta T\}}] \quad \text{..... (8.a)}$$

$$R(t) = (\frac{12}{\pi})^{1/2}[\frac{A_1}{\rho_\upsilon(h_{fg} + \frac{B_1}{Z_1})}] \quad \text{..... (8.b)}$$

The above equations are applied for large superheats for pure liquids and binary mixtures respectively, and

$$A_1 = \Delta T\sqrt{\rho_l\, C_{pl} kt} \quad \text{..... (9.a)}$$

$$B_1 = (y\rho_l - C_\infty)R_g T_S^{\,2}(1-\alpha_S)\sqrt{(\frac{\rho_l C_{pl} k}{D})} \quad \text{..... (9.b)}$$

$$Z_1 = C_\infty h_{fg}[M_2 C_\infty + (\rho_l - C_\infty)M_1][1+\alpha_S h_{fg2}(\rho_l - C_\infty)/h_{fgl} C_\infty] \quad \text{..... (9.c)}$$

Scriven [4], solution implied that the temperature and concentration at the bubble boundary remain constant throughout bubble growth.

Van Stralen [5], extended the theory of Scriven [4] concerning the bubble growth rate in binary mixtures. His model was based on the fact that the bubble growth is accompanied by simultaneous cooling of a superheated liquid microlayer adjacent to the bubble wall. The growth constant for free bubbles was expressed in the form:

$$c_{1,m} = (\frac{12}{\pi})^{1/2} \frac{a^{1/2}}{\frac{\rho_\upsilon h_{fg}}{\rho_l C_{pl}}\{1-(y-x)(\frac{a}{D})^{1/2}\frac{C_{pl}}{h_{fg}}(\frac{dT}{dx})_{x=x_b}\}} \quad \text{..... (10.a)}$$

The bubble radius as a function of time is

$$R(t) = (c_{1,m}\Delta T)t^{1/2} \quad \text{..... (10.b)}$$

The growth rate constant, $c_{1,m}$ is a minimum for a low concentration of the more volatile component in a binary mixture at which the ratio ($\delta T/G_d$) is a maximum. Here, δT refers to the temperature difference between the bulk saturation temperature corresponding to the bulk composition and that at the bubble boundary, G_d is the vaporized mass diffusion fraction. This ratio is calculated graphically from the equilibrium diagram of the binary mixture considered. Van Stralen [6] later suggested introducing a modified Jakob number for binary mixtures to account for the effective temperature driving force in mixtures defined as:

$$J_m = \frac{\rho_l C_{pl}}{\rho_\upsilon h_{fg}}(\Delta T - \delta T) \quad \text{..... (11.a)}$$

Therefore, eq.(3.a) has the following form for binary mixtures:

$$R(t) = (\frac{12}{\pi})^{1/2} J_m (at)^{1/2} \quad \text{..... (11.b)}$$

The modified Jakob number is equal to that of pure liquids and azeotropic mixtures since (δT=0) then.

Han and Griffith [7], developed a model to describe the bubble growth rate in a nonuniform temperature field. They explained the importance of the "waiting period" between the departure of a bubble and the nucleation of another bubble from the same site. During this period, the site and the surrounding area of the heating surface are flooded with bulk liquid. The thermal layer builds up again until the temperature and other conditions at the boiling site are right for nucleation. Bruijn [8], used the same form of eq.(6.a) and eq.(6.b) with ignoring the effect of convection term which results from the change of density accompanying evaporation (ε=0). He represented the bubble radius in the form $R(t)=c_1 t^{1/2}$ for asymptotic growth and constant values of concentration and temperature on the moving boundary, hence c_1 is the bubble growth constant.

Benjamin and Westwater [9], measured the boiling bubble growth rate in mixtures of water/ethylene glycol at atmospheric pressure. The experimental data showed that the variation of R(t) with time had an exponent of (0.4) rather than (0.5) as predicted by Scriven [4]. Yatab and Westwater [10], showed that their experimental data of ethanol/water and ethanol/isopropanol mixtures boiling at atmospheric pressure gave the exponents of (0.32) and (0.27) for the time respectively. Those values were less than the predicted value of (0.5) of Scriven [4].

Many investigators such as Calus and Rice [11], Calus and Leonidopoulos [12], Mikic and Rohsenow [13], and Thome [14], have employed the bubble growth rate, bubble departure diameter with or without nuclei population on the heating surface, to estimate the nucleate boiling heat transfer coefficient and heat flux.

Hence, it is very important to concentrate on the prediction of bubble growth rate as a starting point for understanding the boiling phenomenon. Most of the models used to predict the bubble growth rate reviewed above are restricted by the initial and boundary conditions. To establish a new approach to predict the bubble growth rate in pure liquids and binary mixtures, a moving boundary numerical analysis based on the finite difference scheme was developed in this investigation.

2. Model Statement

The object of the model described in this research is to determine the bubble radius as a function of time in the form, $R(t)=c_1 t^n$. In binary mixtures, the vapor/liquid interface position with respect to a fixed point in space, temperature and concentration can be obtained at any time (t) by using the energy and mass balance equations there. This requires knowledge of the instantaneous temperature and concentration gradients at the interface. To obtain such parameters, instantaneous knowledge of the concentration and temperature at the bubble interface and in the liquid close to the bubble boundary are required. In the mixture case, solution of both

mass diffusion and energy equation are required to do this. For pure liquids, only the temperature gradient at the bubble boundary is required to trace the bubble radius at any time (t), then the solution of only the energy equation is required.

The model of the bubble growth rate is therefore, based on the general equations controlling the heat and mass transfer at the vapor/liquid interface and temperature and concentration distribution in the liquid in the vicinity of the bubble boundary.

3. Mathematical Model

In this model, the bubble is considered to have a spherical shape and symmetrical. Therefore, the temperature and concentration everywhere are only a function of position (r) for any specified time. **Figure (1)** shows the position of the bubble boundary and at a point (i) in the liquid away from the interface at time (t), solid lines, and (t+Δt), dashed lines. Let us assume that the bubble and point (i) radii at time (t) are R(t) and r_i (t) respectively. After a time step (Δt), the bubble expands to radius R(t+Δt). The point (i) has moved to position r_i (t+Δt). The object is to find R(t+Δt) and r_i (t+Δt) in addition to the new temperature and concentration at these positions.

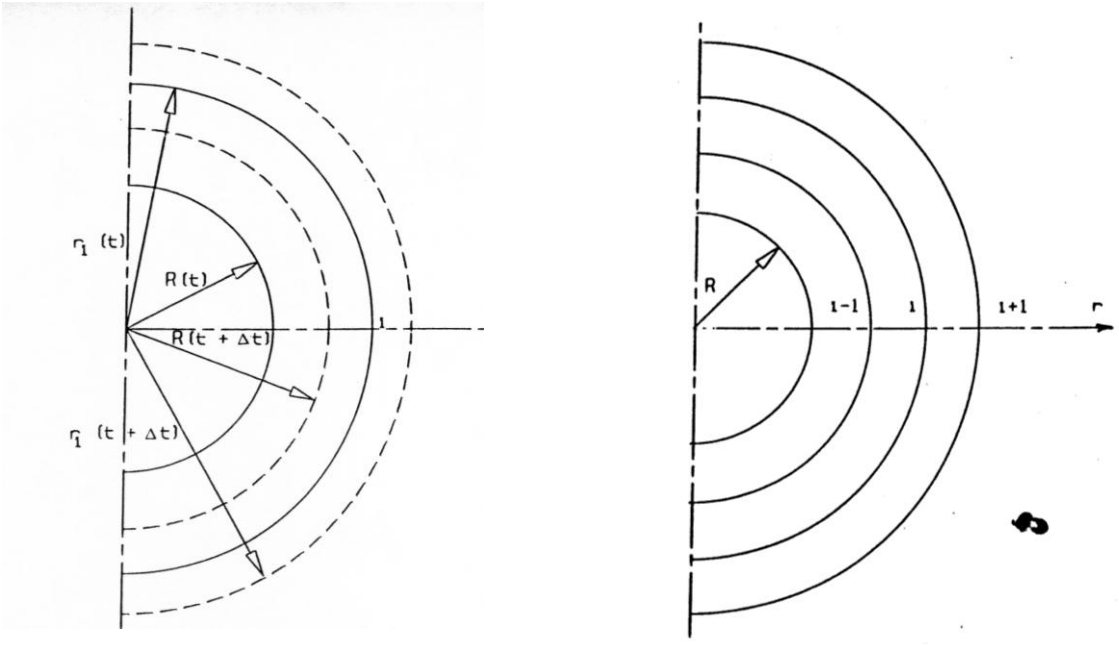

(a) Liquid Velocity Derivation **(b) Finite Difference Scheme**

Figure (1) Bubble Growth Finite Difference Scheme

3-1 Bubble Boundary

The mass balance of the more volatile component at the bubble boundary is expressed by [4] in the form:

$$y\rho_{\upsilon}\dot{R} = C(R,t)(1-\varepsilon)\dot{R} + D(\frac{\partial C}{\partial r})_{r=R} \quad \text{..... (12.a)}$$

which can be transformed for a time step (Δt) as follows:

$$\frac{4\pi}{3\Delta t}\{\rho_{\upsilon}R^3y)_{t+\Delta t} - (\rho_{\upsilon}R^3y)_t\} = 4\pi R^2(t)C_1\{\dot{R} - u(R)\} + 4\pi R^2(t)D(\frac{\partial C_1}{\partial r})_{r=R} \text{ .....(12.b)}$$

The left hand side of the above equation is the rate of change of mass of the more volatile component in the vapor. The first term on the right represents the evaporated mass of the more volatile component due to the density difference between the vapor and liquid phases, convection term. The last term is the mass transfer of the more volatile component due to diffusion.

The energy balance at the bubble interface was derived to avoid any approximation made by Scriven [4], such as constant internal energy and vapor density which are functions of composition in addition to temperature for binary mixtures. It can be written in the form:

$$\Delta U_{\upsilon} = Q_{ev} + Q_{co} - W \quad \text{..... (13)}$$

where (ΔU_{υ}) is the rate of change of the vapor internal energy, (Q_{ev}) and (Q_{co}) are the rate of heat transfer to the bubble due to evaporation and conduction respectively. The last term (W) is the rate of work done on the surrounding liquid due to the bubble expansion during (Δt) time, where:

$$\Delta U_{\upsilon} = \frac{4\pi}{3\Delta t}\{(\rho_{\upsilon}R^3u_g)_{t+\Delta t} - (\rho_{\upsilon}R^3u_g)_t\}$$

$$Q_{ev} = 4\pi R^2(t)\rho_l\{\dot{R} - u(R)\}h_f$$

$$Q_{co} = 4\pi R^2(t)k(\frac{\partial T}{\partial r})_{r=R}$$

and:

$$W = \frac{4\pi}{3\Delta t}\{R^3(t+\Delta t) - R^3(t)\}p_{\infty}$$

The convection term in eqs.(12.b) and (13) can be formulated as a function of the rate of change of the vapor mass during time (Δt) in the form:

$$\frac{4\pi}{3\Delta t}\{(\rho_\upsilon R^3)_{t+\Delta t}-(\rho_\upsilon R^3)_t\}$$

Then, equations (12.b) and (13) can be written in the forms:

$$\frac{4\pi}{3\Delta t}\{(\rho_\upsilon R^3 y)_{t+\Delta t}-(\rho_\upsilon R^3 y)_t\}=\zeta+4\pi R^2(t)D(\frac{\partial C_1}{\partial r})_{r=R} \quad \textbf{..... (14)}$$

and:

$$\frac{4\pi}{3\Delta t}\{(\rho_\upsilon R^3 h_g)_{t+\Delta t}-(\rho_\upsilon R^3 h_g)_t\}=\varphi+4\pi R^2(t)k(\frac{\partial T}{\partial r})_{r=R} \quad \textbf{..... (15)}$$

where:

$$\zeta=\frac{4\pi C_1}{3\rho_l\Delta t}\{(\rho_\upsilon R^3)_{t+\Delta t}-(\rho_\upsilon R^3)_t\}$$

and:

$$\varphi=\frac{4\pi}{3\Delta t}\{(\rho_\upsilon R^3)_{t+\Delta t}-(\rho_\upsilon R^3)_t\}h_f$$

In the present forms of the mass balance, eq.(14), and the energy balance, eq.(15), the mass fraction of the more volatile component, (y), and the vapor internal energy were allowed to vary with time. These equations were solved simultaneously by using the Newton iteration method, to obtain the new vapor composition after time (Δt) and the new radius of the vapor bubble.

Assuming an equilibrium condition between the vapor and liquid at the interface determines the temperature at the bubble boundary which in turn fixes the concentration there. The temperature at the vapor/liquid interface is the saturation bubble point temperature, (T_S) at the bubble wall composition and the ambient pressure, operating pressure of the boiling process. Therefore, the relation between the bubble wall temperature and composition may be presented in the form $T_S(X,p)$.

3-2 Liquid Domain

In the liquid domain, eq.(6.a) and eq.(6.b) must be used to predict the rate of temperature and concentration distribution throughout the liquid in the vicinity of the bubble wall. The temperature distribution in the liquid domain may be written for moving grid line, (*i*), in terms of a position (*i*) fixed in space as:

$$(\frac{\partial T}{\partial t})_i=\frac{\partial T}{\partial r}\frac{dr}{dt}+\frac{\partial T}{\partial t}$$

Therefore, eq.(6.b) may be expressed as:

$$(\frac{\partial T}{\partial t})_i = a\{\frac{\partial^2 T}{\partial r^2} + \frac{2}{r}\frac{\partial T}{\partial r}\} - \frac{\partial T}{\partial r}\{u(r) - v(r)\} \quad \text{..... (16)}$$

To simplify the application of eq.(16), it was decided to move each node with the local velocity of the liquid, $u(r)=v(r)$. Therefore, the last term of eq.(16) is zero. Hence:

$$(\frac{\partial T}{\partial t})_i = a\{\frac{\partial^2 T}{\partial r^2} + \frac{2}{r}\frac{\partial T}{\partial r}\} \quad \text{..... (17)}$$

The above equation was solved for an unequal mesh size, since the nodes were moved with different velocities as a function of position. Therefore, an energy balance over a control volume must be derived for temperature prediction as a function of position and time, $T(r,t)$. Referring to **Fig.(1)**, the energy balance can be written in the form:

$$Q_{i-1\to i} + Q_{i+1\to i} = \Delta Q_i \quad \text{..... (18)}$$

where $Q_{i-1\to i}$ and $Q_{i+1\to i}$ are the heat conduction components from nodes $(i-1)$ and $(i+1)$ respectively. ΔQ_i must equal the rate of change of the internal energy of the liquid in the control volume around the node (i).

The implicit method which is stable for all values of (Δt) and (Δr) was used to derive a formula suitable for prediction of temperature distribution throughout the field considered in the form:

$$T_i = -A_{i-1}T'_{i-1} + (1 + A_{i-1} + A_{i+1})T'_i - A_{i+1}T'_{i+1} \quad \text{..... (19)}$$

where:

$$B_1 = (\frac{\Delta_1}{2} + \frac{\Delta_2}{2}) + \frac{1}{r_i}[(\frac{\Delta_2}{2})^2 - (\frac{\Delta_1}{2})^2] + \frac{1}{3r_i^2}[(\frac{\Delta_1}{2})^3 + (\frac{\Delta_2}{2})^3]$$

$$B_2 = \frac{a\Delta t}{B_1 r_i^2} \qquad A_{i-1} = \frac{B_2(r_i - \frac{\Delta_1}{2})^2}{\Delta_1} \qquad A_{i+1} = \frac{B_2(r_i + \frac{\Delta_2}{2})^2}{\Delta_2} \qquad \text{and} \qquad A_i = 1 + A_{i-1} + A_{i+1}$$

The above equation was applied at the $(N-2)$ nodes in the liquid region of the finite difference scheme.

An analogous equation to that of the energy equation in the system, eq.(19), was derived for the mass conservation in the liquid domain

$$M_{i-1\to i} + M_{i+1\to i} = \Delta M_i \quad \text{..... (20)}$$

where $M_{i-1\to i}$ and $M_{i+1\to i}$ are the mass diffusion components to the control volume whose center is (i) from the neighboring nodes (i-1) and (i+1) respectively. (ΔM_i) is the rate of change of mass of the control volume in equation, where

$$M_{i-1\to i} = 4\pi\{r_i - \frac{\Delta_1}{2}\}^2 D\{\frac{C'_{i-1} - C'_i}{\Delta_1}\}$$

$$M_{i+1\to i} = 4\pi\{r_i + \frac{\Delta_2}{2}\}^2 D\{\frac{C'_{i+1} - C'_i}{\Delta_2}\}$$

and:

$$\Delta M_i = \frac{4\pi}{3}[(r_i + \frac{\Delta_2}{2})^3 - (r_i - \frac{\Delta_1}{2})^3](\frac{C'_i - C_i}{\Delta t})$$

In the above expressions $\Delta_1=(r_i-r_{i-1})$ and $\Delta_2=(r_{i+1}-r_i)$ for node (i) in the domain considered. Substituting these quantities of ($M_{i+1\to i}$, $M_{i-1\to i}$ & ΔM_i) in eq.(20) yields an equation similar to eq.(19) in the form:

$$C_i = -A_{i-1}C'_{i-1} + [1 + A_{i-1} + A_{i+1}]C'_i - A_{i+1}C'_{i+1} \quad \text{..... (21)}$$

Equation (21) is also applied for (N-2) nodes in the liquid region. Here, the coefficients are defined as those in eq.(19) with B_2 expressed as follows:

$$B_2 = \frac{D\Delta t}{B_1 r_i^2}$$

3-3 Initial and Boundary Conditions

The initial temperature at the bubble boundary was set at a value close to the superheated temperature in the liquid in the vicinity of the interface. However, it was found that whatever the bubble boundary temperature was set to, the temperature at the interface rose immediately to a temperature very close to the superheated liquid temperature. The vapor is in equilibrium with the liquid at the bubble boundary and the vapor pressure is the same as that at ($r\to\infty$) for the asymptotic bubble growth stage. The conditions enable us to determine the liquid mole fraction of the more volatile component from a double polynomial fit in the form $T_S(X,p)$. The determination of the liquid mole fraction at the interface provides the concentration, $C_1(R,t)$, there.

In the liquid close to the bubble boundary, it was assumed that the bubble grows in a field initially having uniform superheat and concentration:

$$T(r,0)= T_0 \quad \text{and} \quad C_1(r,0)= C_0 \qquad \text{..... (22)}$$

The above initial conditions together with the boundary conditions at the vapor/liquid interface, eqs.(14 & 15), and those at infinity, eq.(23)

$$T(\infty,t)= T_0 \quad \text{and} \quad C_1(\infty,t)= C_0 \qquad \text{..... (23)}$$

where used in the prediction of bubble radius R(t), temperature distribution T(r,t) and concentration distribution $C_1(r,t)$ in addition to the condition at the bubble wall.

The liquid domain was allowed to extend to (2mm) as an infinity limit and the mesh size, (Δr), was taken as (5 μm).

For pure liquid model, the solution of only the energy equation as presented by, eq.(19), is required. The temperature distribution in the liquid domain is obtained with the boundary conditions for the temperature at the bubble wall and the liquid boundary at infinity:

$$T(R,t)=T_S(p_\infty) \quad \text{and} \quad T(\infty,t)=T_0 \qquad \text{..... (24)}$$

Here, the temperature at the bubble boundary is constant throughout the bubble life and equal to the saturation temperature at the ambient pressure, operating process pressure. The energy balance at the bubble boundary gives:

$$\frac{4\pi}{3\Delta t}[R^3(t+\Delta t)-R^3(t)]\rho_v h_{fg} = 4\pi R^2(t)k\left(\frac{\partial T}{\partial r}\right)_{R(t)} \qquad \text{..... (25)}$$

4. Case Study

In this section, the model described above was used to predict the bubble growth rate of a wide boiling range mixture, such as equimolar n-Pentane/Tetradecene binary mixture at atmospheric pressure, as shown in **Fig.(2)**. The boiling range is defined as the temperature difference between the dew line temperature and boiling line temperature at the liquid molar value. It is equal to (161°C) for the equimolar ($X_{pen.}$=0.5) of the above mixture as shown in **Fig.(2)**.

Tarrad and Burnside [15], predicted the boiling heat transfer coefficient of the above mixture by the existing correlations of Thome [14], Thome [16], Calus and Leonidopoulos [12] and Schlünder [17]. They found that the predicted values are much lower than the measured values during experiments. This was explained as that these correlations based mainly on the assumption that the number of the active sites in boiling mixtures are the molar mean value of pure liquid component boiling points at the same pressure which was not the case during experiments of the above mixture. These correlations are also depends on the theories of bubble growth rate and departure diameter predicted by Scriven or Van Stralen. Therefore, this mixture was used as a

typical mixture where the existing theories of prediction the boiling heat transfer coefficient are highly unreliable under the present forms. Especially for a wide boiling range mixtures and high wall superheats.

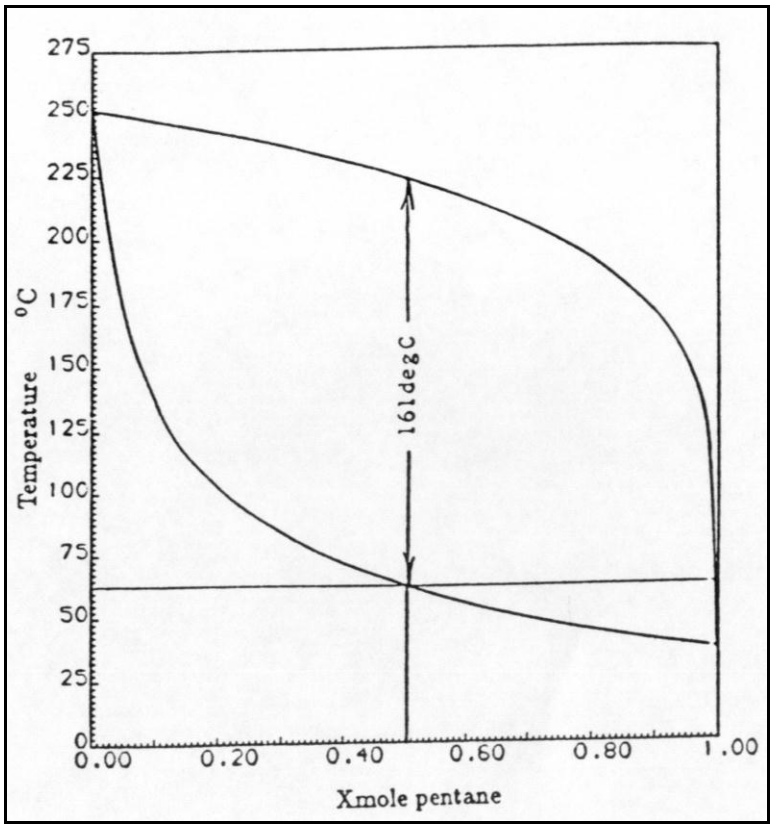

Figure (2) Equilibrium Diagram of n-Pentane/Tetradecene Mixture at Atmospheric Pressure

5. Results and Discussion

5-1 Mixture Model

The bubble growth curve of the equimolar n-Pentane/Tetradecene was predicted for three different superheats, (70, 60 & 50) ^{o}C, as shown in **Fig.(3)**. At all superheats, the initial bubble radius, R(0), and time (t_0) were set to (30 μm) and (1μs) respectively. The initial bubble boundary temperature, T(R,0) was set to a temperature lower than that of the liquid close to the boundary by (0.5 ^{o}C).

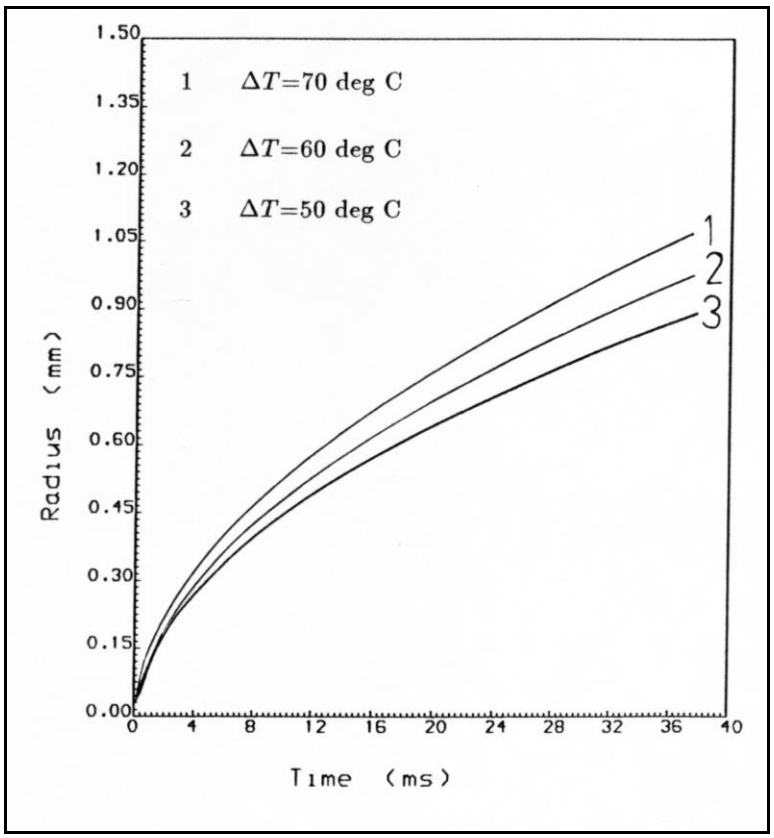

Figure (3) Comparison of Bubble Growth Rate for Equimolar n-Pentane/Tetradecene Mixture

Comparison between the curves in **Fig.(3)** shows that the bubble growth rate increases as the superheat increases. For example, at (t=30 ms), the bubble radii, R(t) at superheats (70, 60 & 50) ^{o}C were (0.94), (0.86), and (0.8) mm respectively. At first sight, it seems that the bubble growth rate was very slow when compared to other more familiar mixtures. This was the main reason for the low boiling heat transfer coefficients obtained when dealing with n-Pentane/Tetradecene mixture. The corresponding figures for the bubble growth constant, $b_1=R(t)/t^{1/2}$, were $(0.54*10^{-2})$, $(0.5*10^{-2})$ and $(0.45*10^{-2})$ respectively, as shown in **Fig.(4)**.

To investigate the effect of mixture composition on the bubble growth rate, the growth curves were obtained for different mole fractions at (Δt= 60) ^{o}C, as shown in **Fig.(5)**. At time (t=30 ms), the predicted bubble radii were (0.76), (0.86), (1.07), (1.13) and (1.2) mm for ($X_{pen.}$=0.4, 0.5, 0.65, 0.7 & 0.75) respectively. These results show that increasing the pentane content of the mixture increases the bubble growth rate.

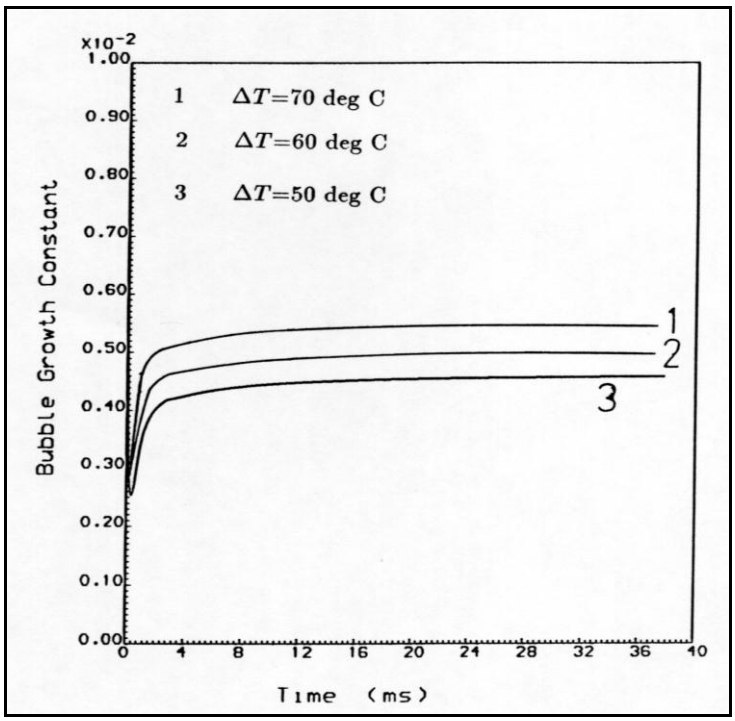

Figure (4) Bubble Growth Constants for Equimolar n-Pentane/Tetradecene Mixture at Different Superheats

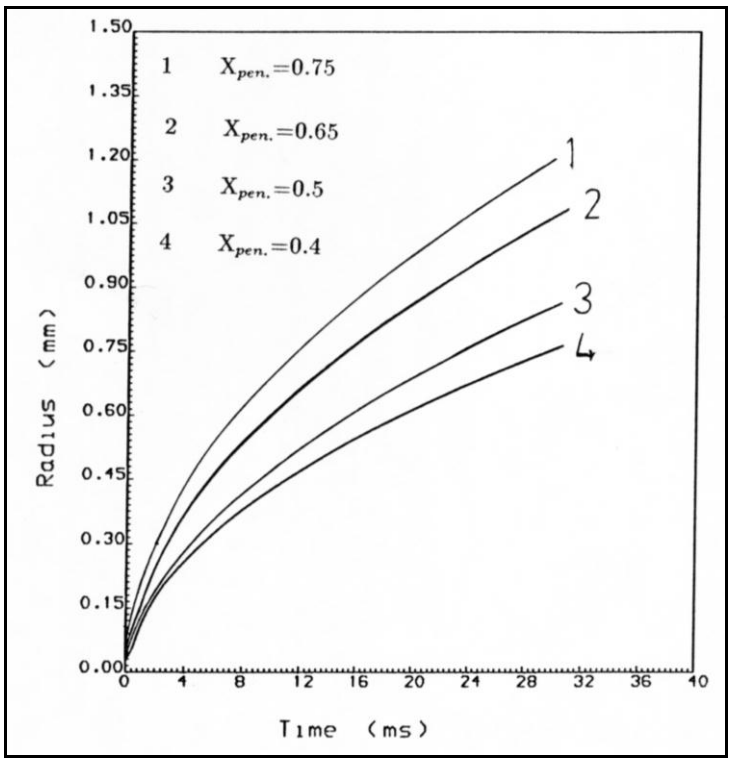

Figure (5) Bubble Radius v. Time for Different Mixture Composition at Superheat of 60 °C

The temperature at the vapor/liquid interface was shown to approach a steady state value which was less than that of the initial superheat only a few degrees, as shown in **Fig.(6)**. **Figure (7)** shows the bubble growth constant, (b_1), for different mixture mole fraction obtained at (ΔT=60) deg C. It is clear that the bubble growth constant (b_1) is nearly constant except in initial bubble growth. This could be due to the assumed initial conditions of temperature and concentration at the vapor/liquid interface and in the liquid in the vicinity of the bubble wall at the end of the inertia bubble growth stage. **Table (1)** shows a comparison of the calculated bubble growth constant, (b_1), with the values of Scriven [4], eq.(8.b) and Van Stralen [6], eq.(11.b).

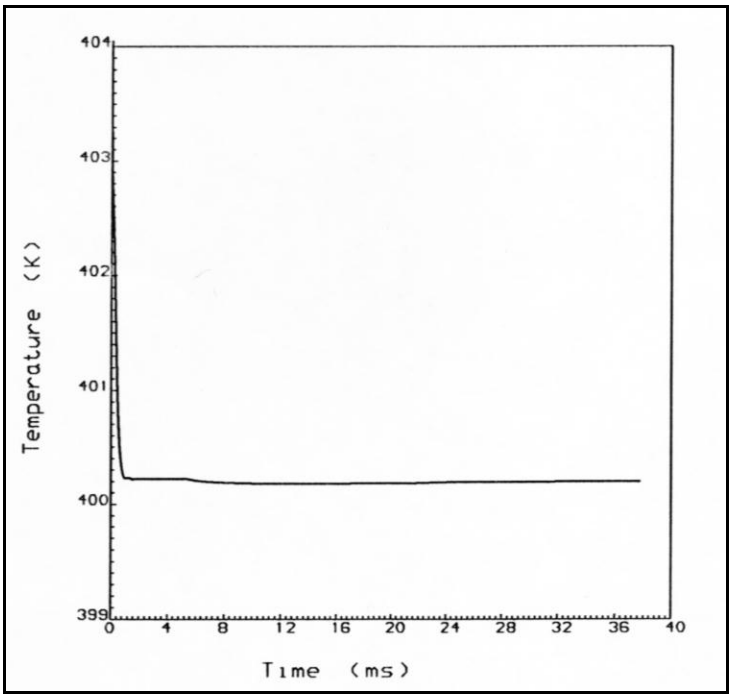

Figure (6) Vapor/Liquid Interface Temperature Variation with Time for Equimolar n-Pentane/Tetradecene Mixture at Superheat of 70 °C

In this table, it can be seen that the predicted values using this analysis are much smaller than those predicted from Van Stralen and Scriven's equations. In fact the latter equations are similar in their forms and prediction. The discrepancy in the bubble growth constant could be explained as follows:

1. The assumption of a linear approximation for the variation of concentration with temperature at the bubble wall in Scriven equation. The equilibrium diagram of n-Pentane/Tetradecene, as shown in **Fig.(1)**, is unlikely to obey this relation.

2. The assumption made by Van Stralen [6] concerning the relation between the composition and the gradient (dT/dX) at the vapor/liquid interface and their values in the bulk to be equal. The present model showed that this assumption is unlikely to be true for the equimolar n-Pentane/Tetradecene mixture.

3. The most sensitive parameter is the superheat (ΔT). Van Stralen and Scriven were allowed the bubble to grow in an effective superheat expressed by ($\Delta T * N_{SN}$) which incorporates the mass transfer effect on the bubble growth rate in the form:

$$N_{SN} = \frac{1}{[1-(Y-X)(\frac{a}{D})^{0.5}(\frac{C_{pl}}{h_{fg}})(\frac{dT}{dX})_{X=X_{bu}}]} \quad \text{..... (26)}$$

The analysis presented here showed that the bubble wall temperature was lower than that in the bulk liquid by only a few degrees. Therefore, the effective superheat expressed by Van Stralen and Scriven is much higher than the actual superheat and overestimate the bubble growth rate in binary mixtures.

The low values of the predicted bubble growth rate could be due a combination of all the above points.

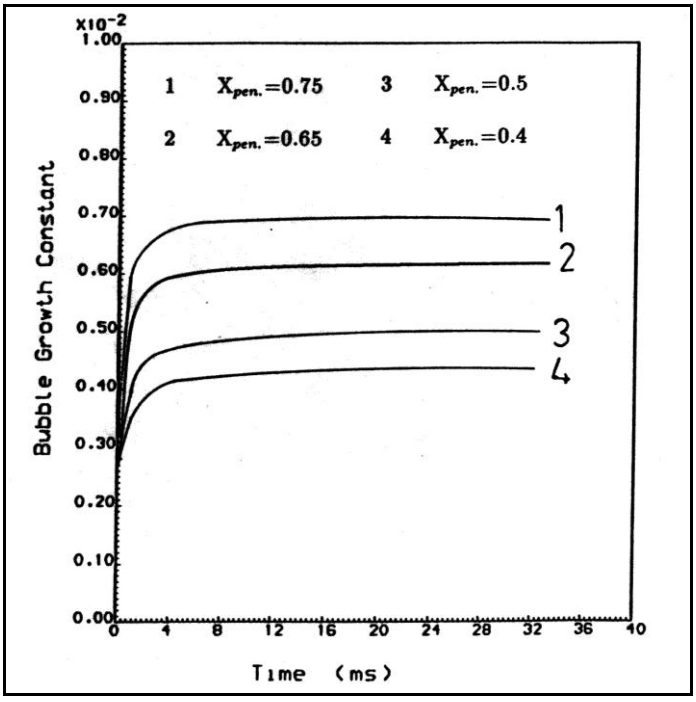

Figure (7) Predicted Bubble Growth Constants for Different Mixture Composition at Superheat of 60 °C

Table (1) Comparison of The Bubble Growth Coefficient With Ref. [4 & 6] at Different Mixture Composition and $\Delta T = 60\ ^{o}C$

$X_{pen.}$	N_{SN}	b_1*10^2 t=30ms	b_1*10^2 Ref. [6]	b_1*10^2 Ref. [4]
0.40	0.42	0.44	2.55	2.40
0.50	0.40	0.50	1.90	2.10
0.65	0.65	0.62	3.46	3.27
0.70	0.59	0.66	3.60	3.35
0.75	0.74	0.69	3.70	3.50

5-2 Pure Liquids Model

The verification of the model presented in this investigation is induced from the application of this model for available experimental data. Solution of eq. (19) of the temperature distribution in the liquid domain together with the boundary conditions presented in eq.(24) predicts the profile of temperature distribution in the vicinity of the bubble wall and liquid field. Equation (25) was solved for the prediction of the bubble radius, R(t) and bubble growth rate. The experiments conducted by Dergarabedian [18], on nucleate pool boiling of water at atmospheric pressure was used at different superheats. Two different superheats, (ΔT=3.1 and 4.5) deg C were used for comparison of the bubble growth rate. The predicted values are well agreed with the available data as shown in **Fig.(8)**. The theory over-predicts the measured bubble radius, the maximum errors were 23% and 12% at superheats of 4.5 and 3.1 deg C respectively. However, the results agree well with Van Stralen's predicted values. In the pure liquid model, the radius at the end of the inertia stage of bubble growth was set equal to 30μm and initial time at both superheats was equal to 1μs.

Figure (9) shows the variation of bubble growth coefficient, β, with time for both superheats. It can be seen that, in the early stages of asymptotic bubble growth , β is a function of time. This could be due to the unknown temperature distribution at the end of inertia bubble growth stage. Later, as the bubble grows, the value of β is essentially independent of time. This indicates that the moving boundary analysis, which makes no initial assumption about the form of variation of R(t) with time, shows that R(t) is indeed varies with $t^{1/2}$ for asymptotic growth of a bubble in an uniformly superheated pure liquid. The β values at the later stages of bubble growth for water superheats of 4.5 and 3.1 deg C were about 13.6 and 9.3 respectively. Compared to β values of 13.2 and 9.1 as predicted from Van Stralen's [6], eq.(11.b) with δT=0, for water superheats of 4.5 and 3.1 deg C respectively.

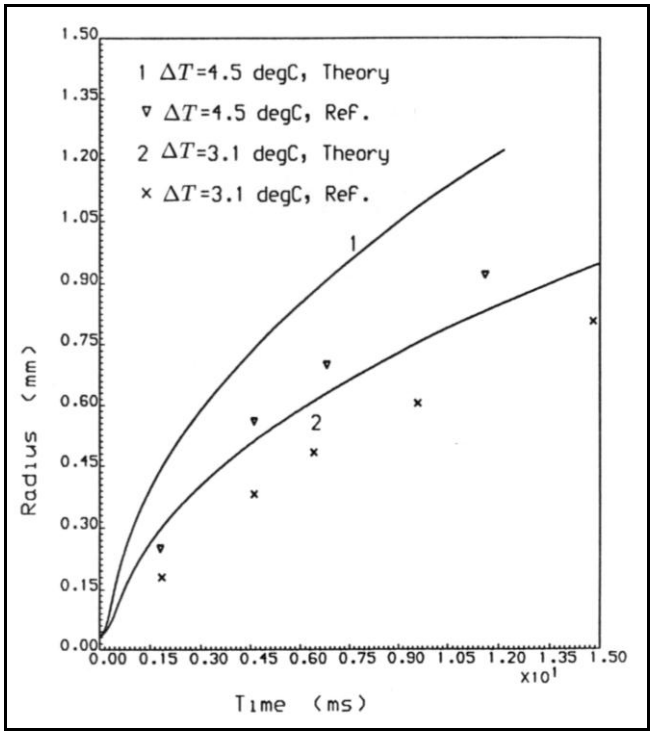

Figure (8) Comparison of Theoretical Bubble Growth Rate with Experimental Data of Dergarabedian [18] Obtained in Water at 1 atm

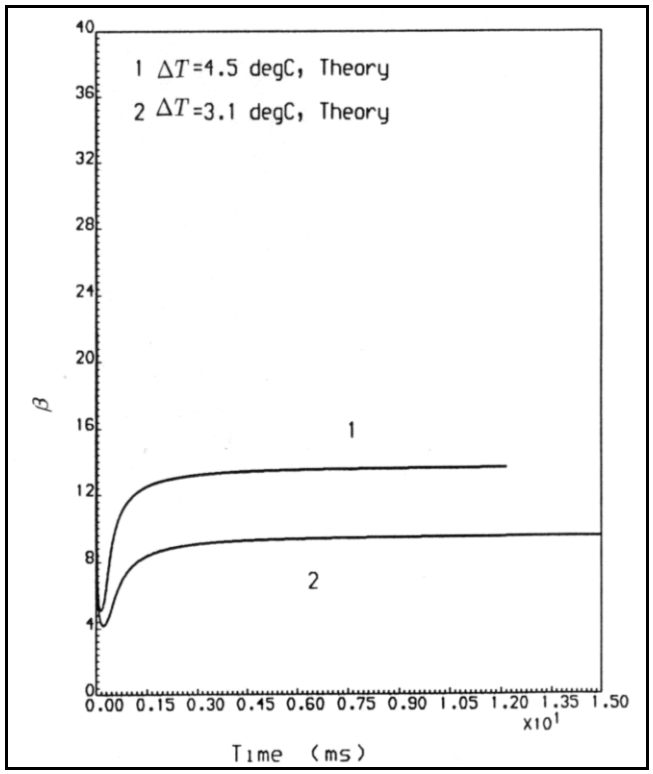

Figure (9) Variation of Predicted Bubble Growth Coefficient with Time for Water Boiling at 1 atm

To show the effect of the presence of the other component on the bubble growth rate of pure liquids and to investigate the response of the model of mixtures and its validity, **Fig.(10)** was prepared. Here, the same wall superheat, $\Delta T=19\ ^{o}C$ was applied for pure n-pentane and ($X_{pen.}=0.95$) for n-Pentane/Tetradecene mixture. The prediction of the mixture model produced lower bubble growth rate than that of pure liquid model as it will be the logical case. This is consistent with other theories where the mixture boiling heat transfer coefficient is always lower than that of pure liquids.

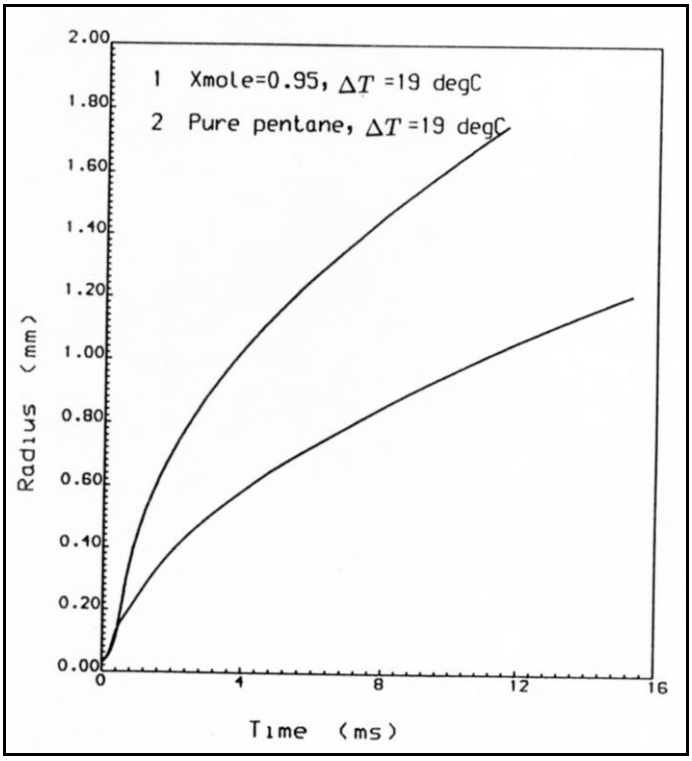

Figure (10) Predicted Bubble Growth Rate of n-Pentane and n-Pentane/Tetradecene Mixture

6. Conclusion

A new approach to the prediction of the bubble growth rate in boiling pure liquids and binary mixtures has been developed. A moving boundary numerical analysis has been applied to the problem in polar coordinates and includes the convection effect due to the density difference between the liquid and vapor phases. Since the effective wall superheat for the bubble growth in binary mixtures is much lower than that the apparent wall superheat, the predicted bubble growth rate for the n-Pentan/Tetradecene mixture was lower than that calculated by the equations of Van Stralen and Scriven. The model which was prepared for bubble growth rate prediction of pure liquids well agreed with available experimental data and that predicted by Van Stralen.

The moving boundary model presented in this investigation for the bubble growth rate prediction of binary mixtures should be tested with existing experimental data for other mixtures. Further, measurements of bubble growth rate for binary mixtures having a wide boiling range are needed.

7. References

1. Rayleigh, L., ***"On the Pressure Developed in a Liquid During The Collapse of a Spherical Cavity"***, Phylosophical Magazine, Vol. 34, pp.94-98, 1917.

2. Plesset, M. S., and Zwick, S. A., ***"The Growth of Vapor Bubbles in Superheated Liquids"***, Journal of Applied Physics, Vol. 25, No. 4, pp.493-500, 1954.

3. Forster, H. K., and Zuber, N., ***"Growth of a Vapor Bubble in a Superheated Liquid"***, Journal of Applied Physics, Vol. 25, No. 4, pp.474-478, 1954.

4. Scriven, L. E., ***"On the Dynamics of Phase Growth"***, Chemical Engineering Science, Vol. 10, Nos. 1-2, pp.1-13, 1959.

5. Van Stralen, S. J. D., ***"The Mechanism of Nucleate Boiling in Pure Liquids and in Binary Mixtures-Parts I & II"***, International Journal of Heat Mass Transfer, Vol. 9, pp.995-1046, 1966.

6. Van Stralene, S. J. D., ***"Bubble Growth Rates in Boiling Binary Mixtures"***, British Chemical Engineering, Vol. 12, No.3, pp.390-394, March, 1967.

7. Han, C., and Griffith, P., ***"The Mechanism of Heat Transfer in Nucleate Pool Boiling-Part I"***, International Journal of Heat Mass Transfer, Vol. 8, pp.887-904, 1965.

8. Bruijn, P. J., ***"On the Asymptotic Growth Rate of Vapour Bubbles in Superheated Binary Liquid Mixtures"***, Physica (S-Grav), Vol. 26, pp.326-334, 1960.

9. Benjamin, J. E., and Westwater, J. W., ***"Bubble Growth in Nucleate Boiling of a Binary Mixture"***, Proc. Conf. Int. Developments in Heat Transfer, Boulder, Univ. of Colorado, pp.212-218, Aug., 1961.

10. Yatab, J. M., and Westwater, J. W., ***"Bubble Growth Rate for Ethanol/Water and Ethanol/Isopropanol Mixtures"***, Chem. Eng. Prog. Symp. Ser., Vol. 62, pp.17-23, 1966.

11. Calus, W. F., and Rice, P., ***"Pool Boiling-Binary Liquid Mixtures"***, Chem. Eng. Sci., Vol. 27, pp.1687-1697, 1972.

12. Calus, W. F., and Leonidopoulos, D. J., ***"Pool Boiling Binary Mixtures"***, Int. J. Heat Mass Transfer, Vol. 17, pp.249-256, 1974.

13. Mikic, B. B., and Rohsenow, W. M., ***"A New Correlation of Pool Boiling Data Including The Effect Of Heating Surface Characteristics"***, Trans. of the ASME., J. of Heat Transfer, pp.245-250, May, 1969.

14. Thome, J. R., ***"Nucleate Pool Boiling of Binary Liquids-An Analytical Equation"***, AIChE. Symp. Ser., No.208, Vol. 77, pp.238-250, 1981.

15. Tarrad, A. H., and Burnside, B. M., ***"Instability in Pool Boiling of a Wide Boiling Mixture on a Horizontal Tube"***, Int. J. of Heat Mass Transfer, Vol. 34, 1991.

16. Thome, J. R., ***"Prediction of Binary Mixture Boiling Heat Transfer Coefficient using Only Phase Equilibrium Data"***, Int. J. Heat Mass Transfer, Vol.26, No.7, pp.965-974, 1983.

17. Schlünder, E. U., Verfahrenstechnik, Vol. 18, pp.692-698, 1982.

18. Dergarabedian, P., ***"Heat Transfer and Fluid Mechanics Institute"***, Paper No.53-SA-10, Los Angeles, California, June, 1953.

Nomenclatures

a : Thermal Diffusivity, (m^2/s)
A : Coefficient in eqs.(19 & 20)
C_P : Specific Heat, (kJ/kg. K)
C_1 : Concentration of More Volatile = Component in Mixture, (kg/m^3)
D : Diffusion Coefficient, (m^2/s)
h_f : Liquid Enthalpy, (kJ/kg)
h_g : Vapor Enthalpy, (kJ/kg)
h_{fg} : Liquid Latent Heat, (kJ/kg)
J : Jakob Number, eq.(3.b)
J_m Modified Jakob Number for Mixtures
K : Thermal Conductivity, (W/m.K)
M : Molecular Weight, (kg/kmol)
N_{SN} : Scriven Number, eq.(26)
P : Pressure, (kPa)

r : Radii Coordinate, (m)
R : Bubble Radius, (m)
$\dot{R}$: Bubble Growth Rate, (m/s)
t : Time, (s)
T : Temperature, (C°)
ΔT : Wall Superheat, (deg C)
x : Mass Fraction of Component in Liquid Mixture
X : Mole Fraction of Component in Liquid Mixture
y : Mass Fraction of Component in Vapor Mixture
Y : Mole Fraction of Component in Vapor Mixture

Subscripts

0 : Initial Value
bu : Value at Bulk Condition
l : Liquid
pen. : n-Pentane Content in Mixture
S : Saturation Value
υ : Vapor
∞ : Value at Infinity
1 : More volatile Component (Solution)
2 : Less Volatile Component (Solvent)

Greek Symbols

α_S : Relative Volatility
β : Bubble Growth Coefficient
δT :Temperature Difference Between Vapor/Liquid Interface and Bulk
ε : Parameter Defined by $(1-\rho_\upsilon/\rho_l)$
ρ : Density, (kg/m^3)
μ : Dynamic Viscosity, ($N.s/m^2$)
ϑ : Specific Volume, (m^3/kg)